Molecular Cell, Volume *28*

Supplemental Data

Ribosome Binding of a Single Copy of the SecY Complex: Implications for Protein Translocation

Jean-François Ménétret, Julia Schaletzky, William M. Clemons, Jr., Andrew R. Osborne, Sigrid S. Skånland, Carilee Denison, Steven P. Gygi, Don S. Kirkpatrick, Eunyong Park, Steven J. Ludtke, Tom A. Rapoport, and Christopher W. Akey

Supplemental Experimental Procedures

Stoichiometry of the ribosome-SecY complex

To determine the stoichiometry, an ~10-fold excess of SecYEG in DBC was added to ribosomes and ~10 pmol of 70S-SecYEG complexes were purified by sucrose gradient centrifugation in 50 mM HEPES-KOH pH 7.5, 100 mM KOAc, 10 mM $Mg(OAc)_2$, 0.3% DBC (Schaletzky and Rapoport, 2006). Peak fractions were identified by A_{260}, pooled, precipitated (Wessel and Flugge, 1984) and resuspended in 20 ul of 50 mM AMBIC containing 10% acetronitrile, then digested with 5 ng/ul of trypsin for 14 hr at 37°C. Aliquots of six AQUA peptides with calibrated concentrations, including one each from proteins L23, L29, and S6 and a peptide from each of the three subunits of the SecY complex, were obtained from Cell Signaling Technology (**Table SII**; the labeled amino acid is underlined and contains both ^{13}C and ^{15}N). For each peptide, the appropriate precursor charge state was determined, along with its optimal fragment ion, collision energy, and detection range. Then 1 pmol of each peptide was added to the digested sample and the mixture was quenched with 20 ul of 50% acetonitrile/5% formic acid. The sample was speed vacuumed to dryness, resuspended in 20 ul of 10% acetonitrile/5% formic acid and half of the mixture was analyzed by liquid chromatography/selected reaction monitoring (LC-SRM) on a TSQuantum Ultra (ThermoElectron, San Jose, CA; Gerber et al., 2003). Peptides were eluted across a 10 minute linear gradient going from a 90:10 to a 80:20 ratio of buffer A (5% acetonitrile, 0.4 % acetic acid, 0.005% heptafluorobutyric acid) to buffer B (95% acetonitrile, 0.4% acetic acid, 0.005 % heptafluorobutyric acid).

All heavy and light SRM transitions are listed in **Table SII**. The parent ions were 2+ peptides and the fragment ions were 1+ peptides, except the RPL23 peptide (2+ fragment). Integrated peak values for light and heavy pairs were extracted from ion chromatograms of the SRM transitions. Masses of the parent and fragment ions were determined using the GPMAW

program (Lighthouse Data). The peak ratio was multiplied by the amount of the heavy internal standard added to the sample (e.g. 1 pmol) to quantitate each native peptide. To check for the consistency of our results, we repeated the experiment with less material and the data from both runs are summarized in **Table SIII**.

Supplemental References

Gerber, S. A., Rush, J., Stemman, O., Kirschner, M. W., and Gygi, S. P. (2003). Absolute quantification of proteins and phosphoproteins from cell lysates by tandem MS. Proc. Natl. Acad. Sci. USA 100, 6940-6945.

Schaletzky, J. and Rapoport, T.A. (2006). Ribosome binding to and dissociation from translocation sites of the ER membrane. Mol. Biol. Cell 17, 3860-3869.

Wessel, D. and Flugge, U.I. (1983). A method for the quantitative recovery of protein in dilute solution in the presence of detergents and lipids. Anal. Biochem. 138, 141-143.

Table S1. Summary of 3D datasets from ribosome-SecY complexes

Ribosome-channel complexes	Sample	†Number of particles	Resolution (FSC 0.5) ribosome and channel
70S-SecY	DDM/carbon film	23,000/28,000	9.6 and 17 Å
70S-SecY¶	DBC/over holes	15,600/19,000	10 and 18.8 Å
70S-tandem SecY	DDM/carbon film	12,000/29,000	22 / nd*
50S-SecY	DDM/carbon film	35,000/63,000	11 and 21 Å

Total particles used/selected : 85,600 /~139,000

†The number of particles in the final maps are indicated, followed by the number of particles that were selected and processed in the refinements.

¶ Data processed with the sep=3 option in EMAN.

* Not determined .

Table S2. Data from a quantitative mass spectrometry analysis of components in the *E. coli* ribosome-SecY complex.

Parent Protein	Peptide Sequence	Heavy SRM Transition	Area Under the Curve	Light SRM Transition	Area Under the Curve	Pmol
RPL23	APH*V*SEK	387.21 ---> 303.2	1881809	384.20 ---> 300.2	4163071	2.22
RPL29	TL*L*NEK	362.72 ---> 510.3	2627712	359.21 ---> 503.3	4143579	1.58
RPS6	FNDA*V*IR	420.73 ---> 579.4	1862606	417.72 ---> 573.3	3718086	2.00
					Ribosome Average	1.94 +/- .32
SECY	L*L*EQQR	397.23 ---> 560.3	1989301	393.72 ---> 560.3	5404808	2.72
SECE	AT*V*AFAR	371.22 ---> 464.3	1324101	368.21 ---> 464.3	3003178	2.26
SECG	GSEWENLSA*P*AK	647.82 ---> 321.2	656222	644.81 ---> 315.2	1387435	2.12
					SecYEG Average	2.36 +/- .32

Note: These data are from experiment 1 with complexes made in DBC.

Table S3. Summary of quantitative mass spectrometry of components in the *E. coli* ribosome-SecY complex in detergent.

Protein component	Experiment 1 (pmoles)	Experiment 2 (pmoles)
rpL23	2.22	1.12
rpL29	1.58	nd
rpS6	2.00	1.08
Ribosome average	1.94	1.10
SecY	2.72	0.77
SecE	2.26	0.83
SecG	2.12	1.00
SecYEG average	2.36	0.86
Ribosome:SecY ratio	0.82	1.27

Note: Different amounts of the complexes were used in the two experiments. However, the overall ratio after combining both experiments is 0.94, very close to 1:1.

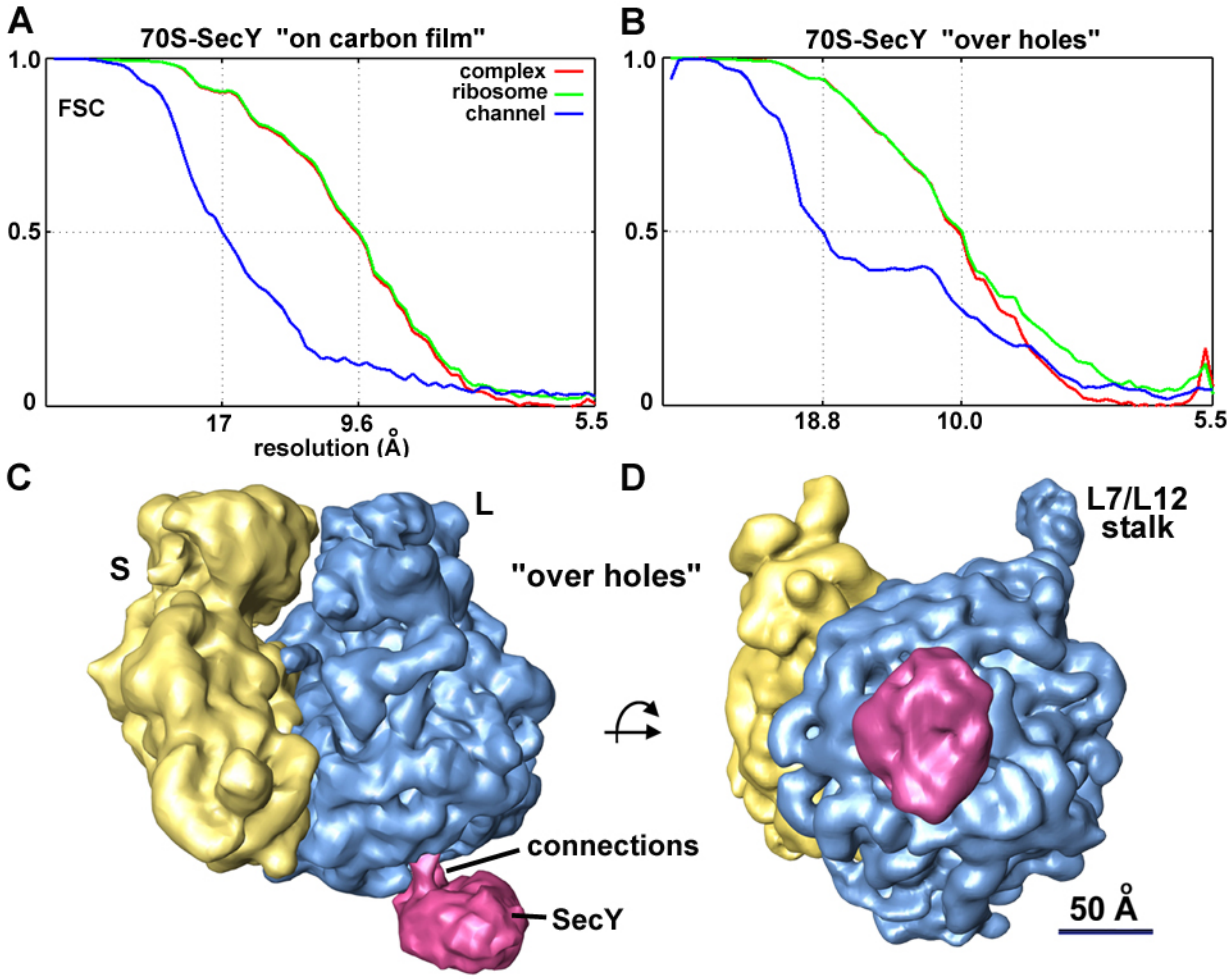

Figure S1. Resolution curves and views of ribosome-SecY complexes.

A. Fourier shell curves are shown for the bacterial ribosome-SecY complex imaged on a carbon film in DDM and the separate components. The curves are color coded.
B. Fourier shell curves are shown for the bacterial ribosome-SecY complex imaged over holes in DBC and the separate components.
C. A front view of a ribosome-SecY complex is shown at 16Å resolution. This complex was imaged over holes in DBC.
D. A bottom view is shown of the ribosome-SecY complex in panel C.

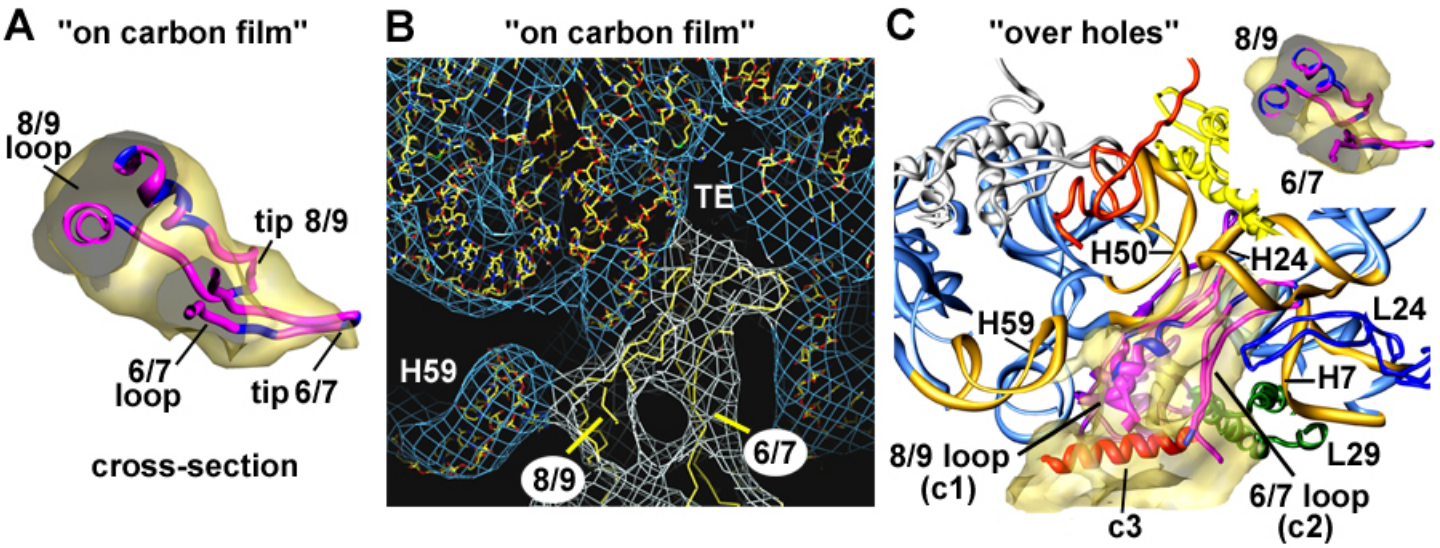

Figure S2. The connections are formed by two cytoplasmic loops of the SecY subunit and the cytoplasmic surface helix of SecE.

A. A close-up is shown of the 6/7 and 8/9 loops (in magenta) within their corresponding density (in yellow) from a 3D map of specimens image on a carbon film. The cut-plane of the cross-sectional view is colored in dark grey. Note that the cross-section for the 8/9 loop is elongated at this level while the corresponding smaller region for the 6/7 loop is triangular. Basic residues are marked in blue.

B. A thin slab is shown of the map density in 'O' from ribosome-SecY complexes imaged on a carbon film. In this view, cytoplasmic loops of the SecY subunit are clearly resolved as two rods that penetrate into a surface depression on the large ribosomal subunit. In addition, H59 interacts with the 8/9 loop. This view is nearly orthogonal to the loops shown in panel A and rotated ~30° counterclockwise.

C. The connections were modeled from a 3D map of ribosome-SecY complexes imaged over holes in DBC. The final model is shown with the important components labeled. The 6/7 and 8/9 loops are magenta with basic residues in blue, while the cytoplasmic helix of SecE is red. (**inset**) A cross-section of the connection density is shown in yellow with the cut-plane in grey.

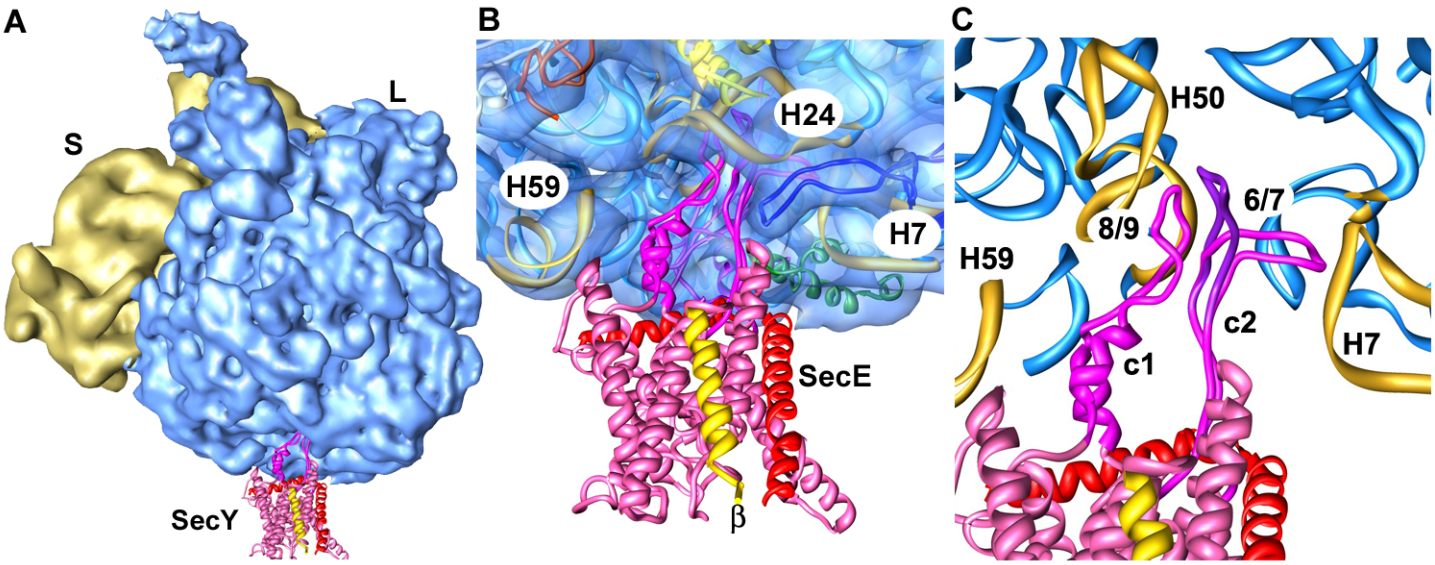

Figure S3. The 6/7 loop of the SecY subunit adopts two alternate conformations at the tunnel exit.

A. An overview is shown of the *E. coli* ribosome with the docked SecY complex.
B. A zoomed in view is shown of the interaction of SecY with the tunnel exit region. The orientation is the same as in panel A.
C. A close-up view is shown of the two modeled conformations for the 6/7 loop, which are colored in magenta and purple. The density for the 6/7 loop suggests that these two conformations may be present in a ratio of roughly 70 (magenta) /30 (purple). The major conformation for loop 6/7 has been used in Figures 3 and S2A. Note that H24 has been removed in this panel for clarity. The major conformation of the 6/7 loop partly blocks the tunnel exit. However, the alternate conformation of the 6/7 loop (shown in purple) may leave a wider opening for the nascent chain when it exits from the tunnel. A structure of a translocating ribosome-SecY complex is needed to investigate this point.